WCTE 2018
2018 World Conference on Timber Engineering
August 20 - 23, 2018 | Seoul, Republic of Korea

NUMERICAL MODELING OF CLT DIAPHRAGMS TESTED ON A SHAKE-TABLE EXPERIMENT

Andre R. Barbosa[1], Leonardo Rodrigues[2], Arijit Sinha[1], Christopher Higgins[1], Reid B. Zimmerman[3], Scott Breneman[4], Shiling Pei[5], John van de Lindt[6], Jeffrey Berman[7], Eric McDonnell[3], Jorge M. Branco[2], Luis C. Neves[8]

ABSTRACT: Current standards and existing literature provide very limited information regarding the design of cross-laminated timber (CLT) floor diaphragms. In addition, limited procedures exist to develop analytical models to estimate the deformation response of CLT floor diaphragms. This paper presents a modelling approach that captures the response of CLT timber diaphragms, with a special focus on CLT spline panel-to-panel connections. The modeling approach is validated through the comparison of the results of the computation model with experimental data obtained from a series of shake-tables test performed on a two-story full-scale building tested in the summer of 2017 at UC San Diego Large High Performance Outdoor Shake Table. The two-story building included two diaphragm designs at each floor level. The first solution consists of CLT panels connected with plywood surface splines that are fastened using self-tapping screws, while the second consists of a CLT-concrete composite floor solution. Results from the nonlinear pushover analysis describe accurately the experimental data obtained.

KEYWORDS: CLT, diaphragms, seismic response, numerical modelling, shake table

1 INTRODUCTION

With the rise in interest in mass timber construction, in North America, researchers and industry practitioners have been involved in advancing the knowledge both in traditional and engineered timber materials. The use of cross-laminated timber (CLT) is increasing due to their proved efficiency in terms of construction approach and aesthetics. One of the key areas of research in this field is tied to the fact that current codes and standards in the United States do not provide guidelines for determining key parameters for design and structural modelling of CLT diaphragms [1,2]. In addition, modelling strategies to estimate the performance of these diaphragms are needed to provide more information with respect to the characterization of CLT floors deformations. Regarding computational modeling of CLT diaphragms, Breneman et al. [3] developed an analysis approach that enabled estimation of deflections and in-plane stress and force distributions, resulting from different design levels of seismic loading. While this analysis approach is promising, there is a need to further refine such tools for design. The development of modelling strategies able to capture complex diaphragms geometries is urgent. In parallel, these new modelling strategies must be validated through comparison of analytical results to experimental data.

This paper presents a series of diaphragm test results measured in full-scale two-story mass timber building shake table testing campaign conducted at the Natural Hazards Engineering Research Infrastructure (NHERI) University of California San Diego (UCSD) (NHERI@UCSD) large outdoor shake table facility, and proposes a methodology for diaphragm design. The diaphragms were designed to sustain the demands of three different testing phases with little to no damage. The three phases were developed to assess the behaviour of three wall lateral resisting systems, including a post-tensioned self-centring rocking wall design (Phase 1), a non post-tensioned rocking wall design (Phase 2), and CLT shear walls with standard nail shear connectors and rod hold-downs (Phase 3). In addition, this paper presents a phenomenological computational modeling approach developed to capture the peak floor deformation response observed during testing. Results regarding the modeling of the diaphragm focus on building response of Phase 1 [4].

[1] Oregon State University, USA, barbosa@oregonstate.edu, arijit.sinha@oregonstate.edu, chris.higgins@oregonstate.edu, leonardofgrodrigues@gmail.com
[2] University of Minho, Portugal, leonardofgrodrigues@gmail.com, jbranco@civil.uminho.pt
[3] KPFF Consulting Engineers, USA, Reid.Zimmerman@kpff.com, Eric.McDonnell@kpff.com
[4] WoodWorks, USA, scott.breneman@woodworks.org
[5] Colorado School of Mines, USA, spei@mines.edu
[6] Colorado State University, USA, jwv@engr.colostate.edu
[7] University of Washington, USA, jwberman@myuw.net
[8] University of Nottingham, UK, Luis.Neves@nottingham.ac.uk

2 CASE STUDY

A 6.7 m tall building structure, shown in Figure 1, was designed, constructed, and then subjected to a series of shake-table tests, at the Natural Hazards Engineering Research Infrastructure (NHERI) University of California San Diego (UCSD) facility, during the summer of 2017. For the three different phases described above the building was subjected to multiple shake table motions replicating historical earthquake ground motion records scaled to different hazard levels: (i) Service Level Earthquake (SLE), (ii) Design Basis Earthquake (DBE), and (iii) Maximum Considered Earthquake (MCE). While special attention was paid to the resilient and innovative wall designs, the floor diaphragms were designed to resist the gravity loads, and to transfer the seismic loads, with minimal damage. The first floor level CLT diaphragm and roof CLT-concrete composite diaphragms have large cantilevered portions that require significant in-plane shear transfer under seismic load. The aspect ratio (1:1) of the cantilevered parts were consistent with the diaphragms built in real buildings.

Figure 1: *Overview of shake-table specimen tested in 2017. The middle floor level consists of a CLT diaphragm. The roof level consists of a CLT-concrete composite diaphragm.*

2.1 DIAPHRAGM DESIGN

The floor level diaphragm consisted of 4.125 inches (104.8 mm) thick 3-ply ANSI/APA PRG 320 V1 grade CLT panels. Panel-to-panel connections are constructed using plywood surface splines with screws, as indicated in Figure 2(a). The chord splices used to resist the diaphragm moments were built with ASTM A36 steel plates fastened to the CLT panels with screws (Figure 2(b)). The roof diaphragm is a 231.8mm CLT-concrete composite floor system [5], consisting of 5-ply V1 grade CLT connected to a concrete topping with self-tapping screws inclined at 45 degrees. Both diaphragms were connected to the walls through an innovative system, shown in Figure 3(a) composed by a steel tongue plate that is connected to a slotted steel plate connection embedded into the CLT panels. Beam-to-beam and beam-to-column connections were executed with steel plates and bolts as shown in Figure 3(b).

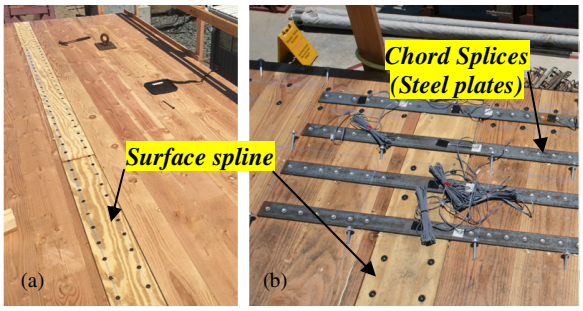

Figure 2: *Diaphragm connections used at the roof: (a) surface splines; (b) chord splices*

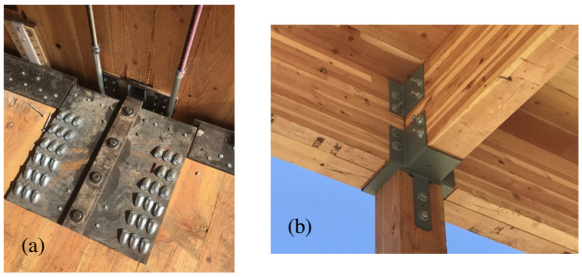

Figure 3: *Floor to lateral and gravity resisting system connection details:(a) diaphragm to wall connection; b) floor to beam-column joint.*

3 DIAPHRAGM SHAKING TABLE TEST RESULTS

3.1 PEAK FLOOR ACCELERATION DISTRIBUTION ELEVATION

An envelope of the diaphragm accelerations measured for the various ground motion records used in the shake table can be observed in Figure 4, where the ratios between the peak floor accelerations (PFA) and the peak shake table accelerations (PGA) are presented for the three phases tested.

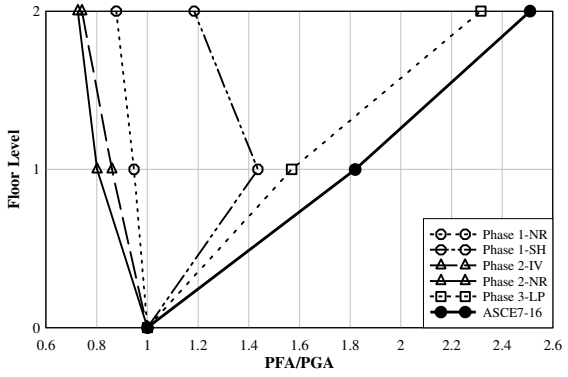

Figure 4: *Peak floor acceleration / Peak ground acceleration ratio for different testing program phases.*

The historical earthquake ground motions used were the following: Northridge, 1994 (NR); Superstition Hill, 1987 (SH); Imperial Valley, 1979 (IV); Loma Prieta, 1989 (LP). Figure 4 also shows the normalized accelerations obtained with the Alternative Diaphragm Seismic Design

Force Level of ASCE 7-16 [6] that were used during the design phase. Results indicate that the lateral resisting system used affects the peak floor acceleration profile. The method proposed in ASCE 7-16 [6] to compute the diaphragm acceleration can be used for conventional shear walls. Nonetheless, in the case of rocking walls the method available in of ASCE 7-16 fails to predict the distribution in height of the diaphragm accelerations.

3.2 PEAK FLOOR ACCELERATION DISTRIBUTION IN PLAN

In order to evaluate the response during earthquakes the accelerations were measured at different locations within each diaphragm. Figure 5 shows the accelerations measured at the center of the diaphragms and at the cantilever parts.

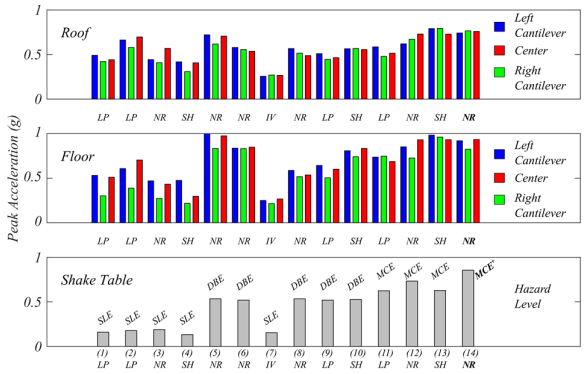

Figure 5: *Peak accelerations measured at different levels and diaphragm positions*

The applicability of the modelling approach proposed in this paper is evaluated using the experimental results obtained during Phase 1 when the structure was subjected to the Northridge, 1994 earthquake presented in Figure 6. This earthquake motion contains the highest peak ground acceleration since it was scaled to exceed the MCE level.

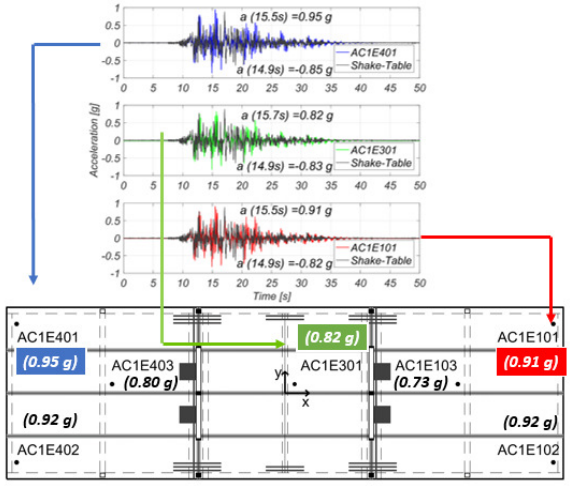

Figure 6: *In-plan distribution of diaphragm acceleration at floor level.*

At the floor level, accelerations at the cantilevered ends was 13 % larger than the ones measured in the centre of the building. Figure 7 shows the in-plan distribution of the diaphragm accelerations at roof level where it can be seen that the CLT-concrete composite responded as a rigid diaphragm. Comparing the results for both diaphragms, it is evident that the floor diaphragm requires more attention, since the accelerations are higher than the ones obtained at the roof. Consequently, the modelling approach proposed here will use the floor diaphragm as case study.

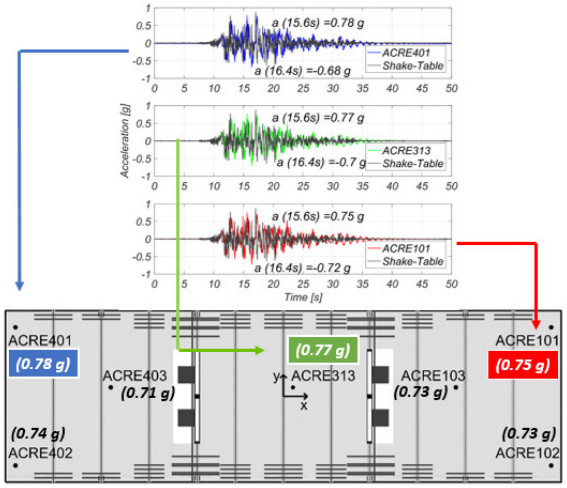

Figure 7: *In-plan distribution of diaphragm acceleration at roof level.*

3.3 DIAPHRAGM DEFORMATIONS

The measurements used to evaluate the accuracy of the modelling approach refer also to ground motion used in Figure 6-7. In Figure 8, the maximum deformations of a single surface spline are presented for both in-plan directions. These values are associated with a maximum inter-story drift ratio equal to 8.4 %. It is worth noting that the measured deformations at surface splines indicate that the separation between panels was very small, eventually smaller than the gap between adjacent panels.

4 MODELLING APPROACH

The proposed modelling approach makes use of shell elements, frame elements, and nonlinear springs representing the connectors. The CLT panels are modelled as orthotropic four-node shell elements, the supporting frame of glulam beams are modelled as elastic frame elements, and the connections to the building lateral resisting elements as fully constrained rigid beam elements. Figure 9 presents the orientation of the major strength direction of the sixteen panels used at the floor level. In addition, the details of the finite element are shown in Figures 9(b) and 9(c).

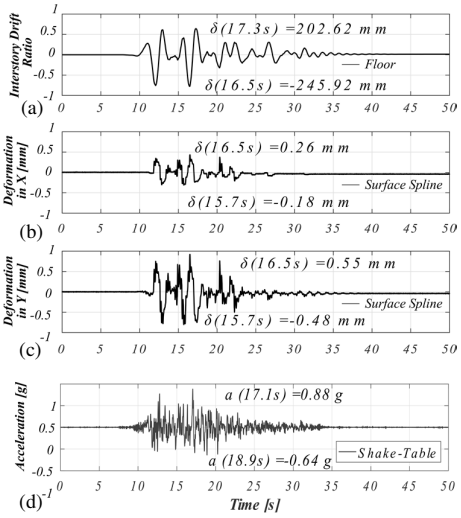

Figure 8: *Diaphragm experimental results: a) inter-story drift ratio; b) surface spline deformation in Y direction (tension-compression); c) surface spline deformation in X direction (shear); d) shake-table accelerations*

4.1 MECHANICAL PROPERTIES OF THE CLT PANELS

The CLT panels used in both diaphragms consist of V1 grade panels per ANSI/APA PRG 320. The floor diaphragm consists of 3-ply CLT, 4.125 inches (104.8 mm) thick. The stiffness properties of single layers were considered through composition factors according to the composite theory proposed in [8]. In addition, the contribution of cross layers was considering when calculating the stiffness in both directions.

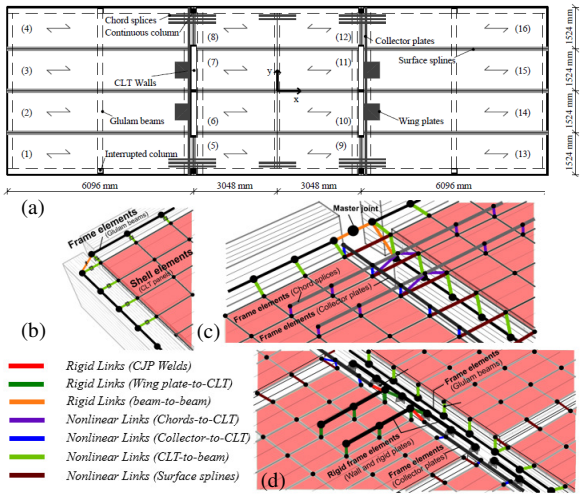

Figure 9: *Finite element model details: a) diaphragm layout; b) beam-to-beam at diaphragm corner; c) chord splice over surface-spline connection; d) diaphragm-to-wall connection*

The method used to estimate the in-plane shear modulus is presented in [9]. This method considers two main mechanisms: (i) shear in single boards and (ii) local torsional moment in the gluing interfaces. Moreover, it is applicable for CLT panels with layers that have the same thickness and similar lumber properties in different cross layers. It was assumed that the lumbers used in different layers have the same mean shear modulus. This is a simplification since the panels were manufactured with Douglas-fir No.2 and Douglas-fir No.3 lumbers in perpendicular directions. The work presented in [9] also proposes different correction factors for 3-ply and 5–ply CLT panels. The main conclusions presented in [10] indicate that the global mechanical behavior of CLT panels can be accurately described using an orthotropic, homogenized, linear elastic material model. The present paper focus only on the in-plane behavior. Nevertheless, the shell element enforces the attribution of E_z, G_{yz} and G_{xz}. Thus, the ratios E_x/E_z, E_x/G_{yz} and E_x/G_{xz} observed in [10] were assumed to compute those properties.

Table 1: *CLT panels mechanical properties*

Prop. *[MPa]*	Value	Notes
E_x	7461.9	Elastic Modulus in the major strength direction ([8])
E_y	3462.8	Elastic Modulus in the minor strength direction ([8])
E_z	500	Elastic Modulus perpendicular to plane ([4], [10])
G_{xy}	575.7	Diaphragm in-plane shear modulus ([9])
G_{yz}	483.3	Out-of-plane shear modulus ([10])
G_{xz}	84.8	Out-of-plane shear modulus ([10])

4.2 CONNECTIONS BEHAVIOR

The values of stiffness and strength were based on the work presented in [11]. However, both the CLT panels and screws tested in [11] were not the same as the ones used in the shake-table test. In addition, the screws used in [11] have a different diameter and tensile strength than those studied in this work. These differences affect the slip modulus (strongly related with timber density) and yielding force of screws (strongly related to embedment strength of timber and screws yielding bending moment). In order to adapt the force-deformation curve per screw obtained in [11] to an envelope curve that can be used to represent the connections built in the diaphragm under study, two different correction factors are here proposed. The first correction factor (λ_K) is used to multiply the stiffness obtained in [11] and is given by the following ratio:

$$\lambda_K = \frac{K_{ser,con}}{K_{ser,dyn}} \quad (1)$$

where K_{ser} is the slip modulus prescribed in EC5 [12] for timber-to-wood based panels connections. Thus, $K_{ser,con}$ is the slip modulus obtained with properties of the materials used at the shake table test, and $K_{ser,dyn}$ is the slip modulus computed with the properties of the material used in [11]. The second correction factor (λ_F) is used to multiply the strength (forces) that defines the force-deformation curve obtained in [11]. The factor λ_F is given by the ratio:

$$\lambda_F = \frac{III_{s,con}}{III_{s,dyn}} \quad (2)$$

where III_s is the force associated to the failure mode that implies fastener yield in bending at one hinge and bearing-dominated yield of plywood fibers (side element) in

contact with the fastener. This force was determined according to [12] with properties of the materials used at the shake table test ($III_{s,con}$), and the properties of the materials used in [11] ($III_{s,dyn}$). The same approach was considered to compute the force-deformation response (per screw) associated to CLT-to-beam connections and steel-to-CLT connections (chord splices and collector plates). The results obtained are presented in Table 2, where force-displacement values are presented for the notable nodes shown in Figure 10 b). The friction between surfaces implies that the screws develop their work only when the force applied exceeds the static friction force (F_μ). This friction force is dependent on the structural weight and on the clamping force (F_c) applied when the screws were fastened (Figure 10 a)). The clamping forces values are uncertain given that the assemblage of the structure was performed without using any torque specification during screws installation. In fact, the construction workers simply ensure that the connector is tight and fully installed. In the scope of the present work, two levels of clamping force (F_c) were assumed, $0.1F_I$ and $0.2F_I$. Moreover, three different levels of static friction coefficient were considered: 0.3, 0.4 and 0.5. The determination of static friction force (F_μ) is given by:

$$F_\mu = (W + F_c) \cdot \mu \quad (3)$$

Table 2: *Points used to define the force-deformation response (per screw) for the diaphragm connections.*

Point	*Connection*	F_i *(N)*	δ_i *(mm)*
I	Surface splines[a]	936.8	1.4
II		3145.8	10.1
III		4126.3	27.4
I	Surface splines[b]	1001.4	1.40
II		3268.5	8.53
III		4287.2	15.17
I	Chord splices & Collector plates[c]	1828.3	1.26
II		5967.5	7.66
III		7827.5	13.63
I	CLT-to-beam[d]	2436.2	3.75
II		7951.5	22.79
III		10429.9	40.52

[a] Performance of CLT connections [11]: Myticon ASSY 3.0 Ecofast Screws SDW22338 TRUSS/EWP PLY

[b] Shake Table Test: Simpson Strong Tie SDW22338 TRUSS/EWP PLY

[c] Shake Table Test: Simpson Strong Tie SDS25312 HEAVY-DUTY CONNECTOR

[d] Shake Table Test: Simpson Strong Tie SDWS22800 LOG

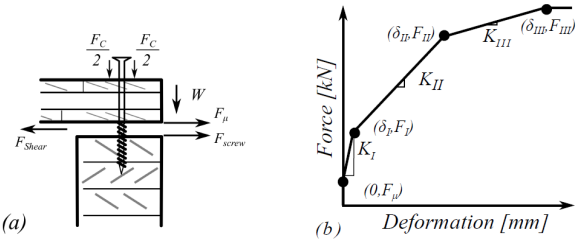

Figure 10: *Friction modelling: a) CLT-to-beam example of forces transfer; b) force-deformation response envelope;*

5 NUMERICAL RESULTS

The diaphragm response is studied here through nonlinear pushover analysis, where all loads are applied incrementally from zero to the full-specified magnitude. Each nodal load has a magnitude equal to the product of nodal tributary mass and the diaphragm acceleration determined for that specific coordinate. The accelerations considered were obtained during Phase 1 for the Northridge, 1994 earthquake scaled for the MCE level. The floor level diaphragm accelerations considered are presented in Figure 6. The diaphragm deformations obtained from the pushover analysis are presented in Figure 11. It is worth noting that the walls were simulated using rigid beams with fully constrained nodes. Thus, the displacements presented in Figure 11 refer to relative displacements between walls and floor nodes.

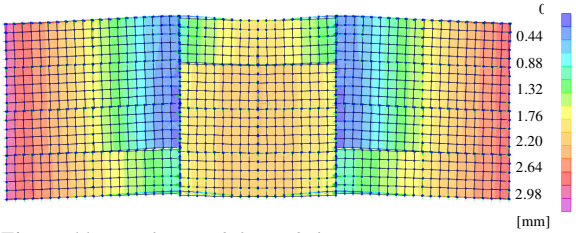

Figure 11: *Diaphragm deformed shape*

5.1 INFLUENCE OF FRICTION FORCES

In terms of relative displacements between CLT panels, the numerical analysis results approximate with good accuracy the measurements obtained experimentally. For clarification purposes, the henceforth nomenclature used is C0XXFRYY, where XX is the percentage of the force (F_I) used to model the clamping force (C0) and YY is relative to the friction coefficient (FR) considered (μ=0.5 corresponds to YY=05). The results presented in Figures 10-12 allow assessing the importance of modelling friction while calibrating numerical models to experimental results. Figure 12 presents the separation between two adjacent panels, where it is visible its nonlinear behavior. Figure 13 presents the sliding along a surface spline longitudinal direction. The experimental results indicate that friction can play a crucial role on the performance of the surface splines.

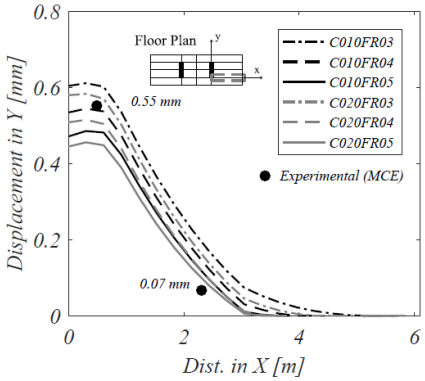

Figure 12: *Numerical results: surface spline separation*

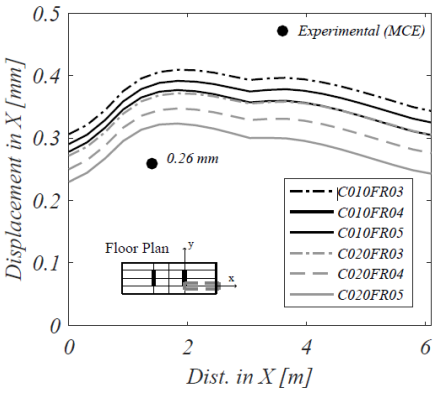

Figure 13: *Numerical results: surface spline deformations in longitudinal direction*

Figure 14 presents the results obtained for a connection between CLT panels and glulam beams. It is worth nothing that these connections have higher friction forces per length, given the gravitational loads transfer, than the surface splines. In this case, the friction force has a lower impact on the connections deformation.

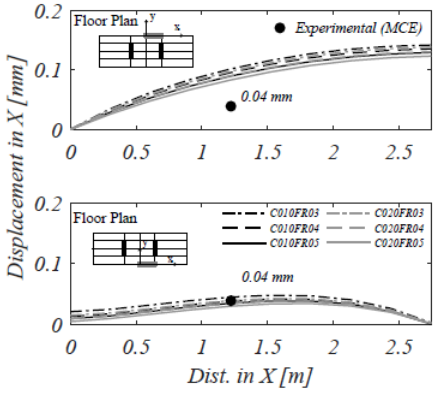

Figure 14: *Numerical results: panel-to-beam deformations in longitudinal direction*

The inclusion of friction on the numerical models can be a burdensome task. It involves the computation of the vertical loads transmitted between connections and the assignment of values for several nonlinear link properties, given the differences on the weight transferred from connection to connection. By including friction forces on the force-displacement response of connections, the numerical model conducts to an over prediction of deformations in the panels, which is acceptable for design in terms of forces in connectors. Nevertheless, a numerical model that neglects friction produces conservative results in terms of surface spline forces and chord splices forces as well. This feature is appealing in design situations involving quick decisions. The results presented in Figure 15 refer to the surface spline that had higher displacements during the shake-table test. The consideration of friction implied a reduction of 11.4 % on the maximum load in the longitudinal direction (Figure 15 a)). For the tension forces, perpendicular to the surface spline, the inclusion of friction produced a decrease of 39.8%.

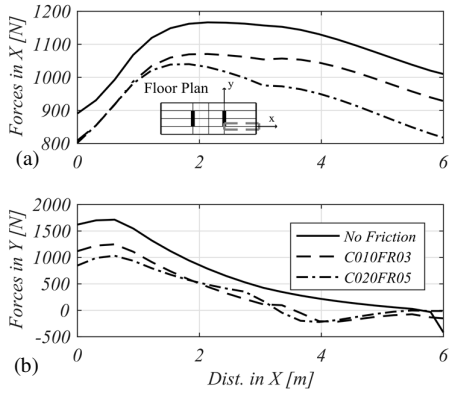

Figure 15: *Effect of friction in surface spline forces: a) shear; b) tension-compression*

The consideration of friction implies also a reduction on the chord splice forces, as presented in Table 3. It is worth noting that the experimental chord splice stresses were obtained by multiplying the strains measured in situ by the elastic modulus of an ASTM A36 steel (200 *GPa*). Thus, the chord forces were obtained by multiplying the stresses by the cross-section area.

Table 3: *Chord splice forces for Northridge (1994) earthquake scaled for MCE level.*

Steel Plate	*Environment*	*P(N)*	*Total Chord Force (N)*
Top		16189.3	38699.6
Middle	Experimental	11416.4	
Bottom		11093.9	
I	Numerical	3992.9	6453.9
II	Model[a]	2461.0	
I	Numerical	3307.7	5867.7
II	Model[b]	2560.0	

[a] No friction considered for nonlinear links
[b] Friction Considered: C020FR05

The discrepancies obtained between experimental and numerical values for the chord splices forces can be

justified by the relative vertical displacements observed in adjacent panels (center and cantilever) during the shake-table test. These occurrences may induce additional normal stresses due to bending of chord plates. Such phenomenon is not captured by the design oriented modelling approach described in the present work.

The influence of in-plane stiffness is assessed in Figure 16. A variation of 10 % in the mean values of lumber elastic and shear modulus was considered in this study. Despite the correlation between elastic and shear modulus [12], these values were evaluated separately.

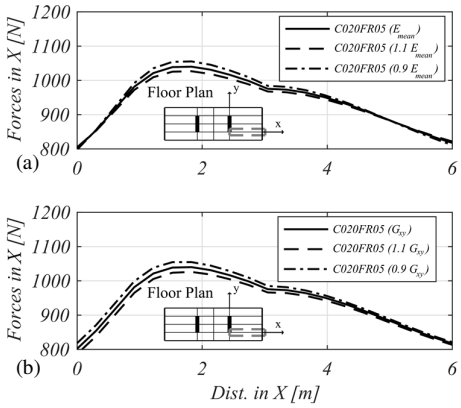

Figure 16: *Surface splines forces along the longitudinal direction: a) influence of elastic modulus; b) influence of in-plane shear modulus*

The model used for in-plane stiffness evaluation considered clamping forces equal to $0.2F_1$ (see Table 2) and a coefficient of friction of 0.5. A reduction on the stiffness properties implies an increase of the surface spline force. Nevertheless, the variation on the surface splines maximum shear forces is equal to 1.5% for both cases presented in Figure 14.

6 CONCLUSIONS

This paper presents a series of diaphragm test results measured in full-scale two-story mass timber building shake table testing campaign conducted at the Natural Hazards Engineering Research Infrastructure (NHERI) University of California San Diego (UCSD) (NHERI@UCSD) large outdoor shake table facility, and proposes a methodology for diaphragm design. The accelerations measured at the diaphragm levels showed that a composite CLT-concrete solution presents a rigid behavior whereas the CLT solution presents higher differences regarding acceleration within the diaphragm. The modelling approach presented in this work refers to the solution built only with CLT panels. The numerical results presented confirm that the approach is able to describe accurately the experimental data obtained from the shake table test. In addition, the inclusion of friction in the force-deformation curves, used to represent the connections, was determinant to achieve a calibrated model in terms of displacements. The modelling approach chosen showed that it can be applied successfully to different diaphragm configurations. One recommends that the mesh is as regular as possible and minimum element length is equal to 1 ft (304.8 mm). The consideration of friction can guarantee a reduction of connectors to be used in surface splines and chord splices.

REFERENCES

[1] S. Pei; D. Rammer; M. Popovski; T. Williamson; P. Line; J. W. van de Lindt. An Overview of CLT Research and Implementation in North America. In: World Conference on Timber Engineering, WCTE 2016. 22-25 August 2016; Vienna, Austria. 10 pp.

[2] K. Spickler, M. Closen, P. Line, and M. Pohll, “Cross Laminated Timber Horizontal Diaphragm Design Example”. White paper, August 2015.

[3] S. Breneman; E. McDonnell; R.B Zimmerman. An Approach to CLT Diaphragm Modeling for Seismic Design with Application to a U.S. High-Rise Project. In: World Conference on Timer Engineering, WCTE 2016. 22-25 August 2016; Vienna, Austria. 9 pp.

[4] S. Pei; J. W. van de Lindt; A. Barbosa; J. Berman; E. McDonnell; J. Dolan; R.B Zimmerman; R. Sause; J. Ricles, K. Ryan Shake-Table Test 2017. In World Conference on Timber Engineering, WCTE 2018. 20-23 August 2018; Seoul, South Korea. 6 pp.

[5] C. Higgins; A.R. Barbosa; C. Blank. “Structural Tests of Concrete Composite-Cross-Lamintated Timber Floors,” School of Civil and Construction Engineering, Corvallis, OR 97331, United States, Rep. no. 17-01, December, 2017, 76 pp. Available http://cce.oregonstate.edu/sites/cce.oregonstate.edu/files/pdfs/som_report_osu_1701.pdf.

[6] S. Ghosh. “ Alternative diaphragm seismic design force level of asce 7-16”. Structure Magazine. March 2016. pp 18-23.

[7] CSI. SAP2000 User’s Manual – Version 19. Computers and Structures, Inc., Berkeley, California. 2017.

[8] H.J Blass; and P. Fellmoser. Design of solid wood panels with cross layers. In World Conference on Timber Engineering, WCTE 2004. 14-17 June 2004; Lahti, Finland. 6 pp.

[9] T. Bogensperger; T. Moosbrugger; G. Silly. Verification of CLT-plates under loads in plane. In World Conference on Timber Engineering. 20-24 June 2010; Riva del Garda, Italy. 10 pp.

[10] D. Gsell; G. Feltrin; S. Schubert; R. Steiger and M . Motavalli. “Cross-Laminated Timber Plates: Evaluation and Verification of Homogenized Elastic Properties ”. *Journal of Structural Engineering,* 133(1), 132-138.

[11] M. Closen. “Performance of CLT connections under dynamic loading”. Available in http://www.my-535ti-con.com/resources/slides-clt-connections-dyn-loading-usa.

[12] AWC. National Design Specication for Wood Construction. Leesburg, VA, 2015.

[13] J. Kohler; J. D. Sørensen and and M. H. Faber. “Probabilistic modeling of timber structures.” Structural Safety, 29(4), 255–267.